CHAPTER 4

Assembling of Inner Part of Belle II CDC

The core structure of the small cell chamber, consisting of CFRP inner cylinder and two aluminum endplates, were made with precise arrangement by engineers of the lab. In this chapter, the assemble and several mechanical tests of the inner chamber are explained. It starts with the assemble and the tension load test of the core structure. Then, the wire stringing and the wire tension check are described. The low tension wires were re-strung to the proper tension. Lastly, the chamber, with the complete wire strung, was inserted in to temporary cover for the gas leak test. The result of gas leak rate modification is also presented.

4.1 Core Structure Assembling and Tension Load Test

The core structure components of the small cell chamber machining and drilling were finished in 2012. By accurate alignment, the front end and the back end endplates as well as the CFRP inner cylinder were mounted by bolts and the connections were covered by aluminum alloy ring. The dislocation of the boundary wire hole position (r,ϕ) between inner and main chamber was less than 100 μm. Then, the thin aluminum films of 0.1 mm thickness were glued on the outer surface of the inner cylinder for electric shield.

The inner cylinder was typically used to supported at least 371.2 kg of wire tension. To avoid the distortion of the core structure, the load capability was tested before the wire was strung. Totally ten pieces of 3.0 mm diameter stainless steel bars, with the screw edge and the spring of steel of a known spring constant, were mounted into the sense wire holes on the 5th layer, as shown in Figure 4.2. Then, the nut was carefully down to increase the tension. The length between the edges of the front end and the back end was measured with two micrometers, fixed on opposite sides of the chamber. Differences of the lengths before and after doing the nut (ΔD) were used to calculate tension on the bars.

Table 4.1: Tension load test result. ΔD is the length difference between before and after applying the tension (mm) at the chamber azimuth angles of 0^o and 180^o.

Tension (kg)	$\Delta D\ 0^o$	$\Delta D\ 180^o$
0	0	0
92.8	0.009	0.011
185.6	0.039	0.049
278.4	0.081	0.089
371.2	0.095	0.108
408.3	0.124	0.135

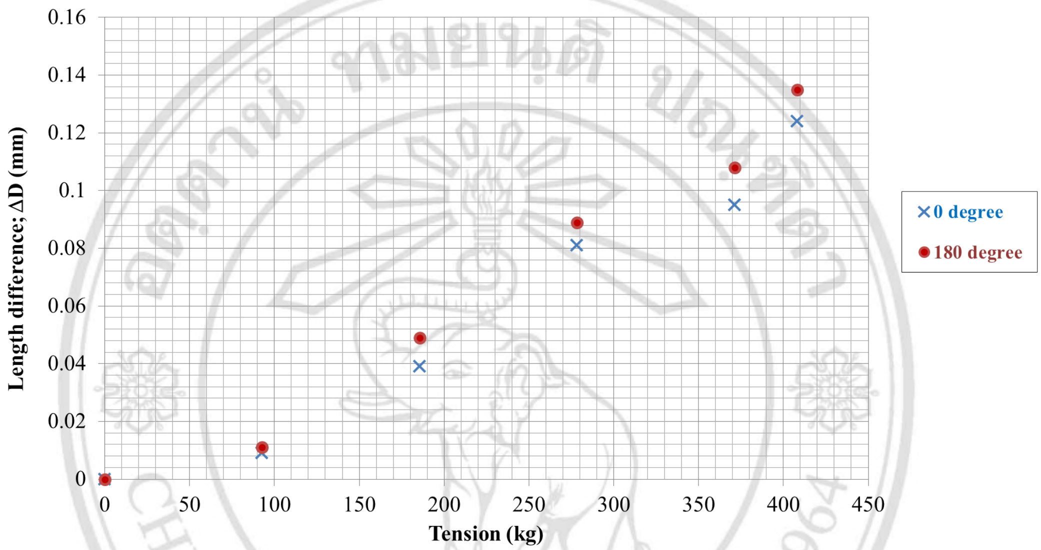

Figure 4.1: Plot of the length difference between before and after applying the tension (mm) as a function of the tension (kg).

The calculated tensions of the bars varying with length of the spring are listed in Table 4.1. Plot of ΔD is shown in Figure 4.1.

The results show that the both endplates can support the tension up to 408.3 kg without buckling. The ΔD while applying the tension of 370 kg was about 0.1 mm. It is corresponding to 0.098 mm of the expected distortion from calculation by the Finite Element Method. After the load test, the bars were still mounted on the chamber with the tension of around 180 kg. When the wire stringing of its layer was started the bars were removed.

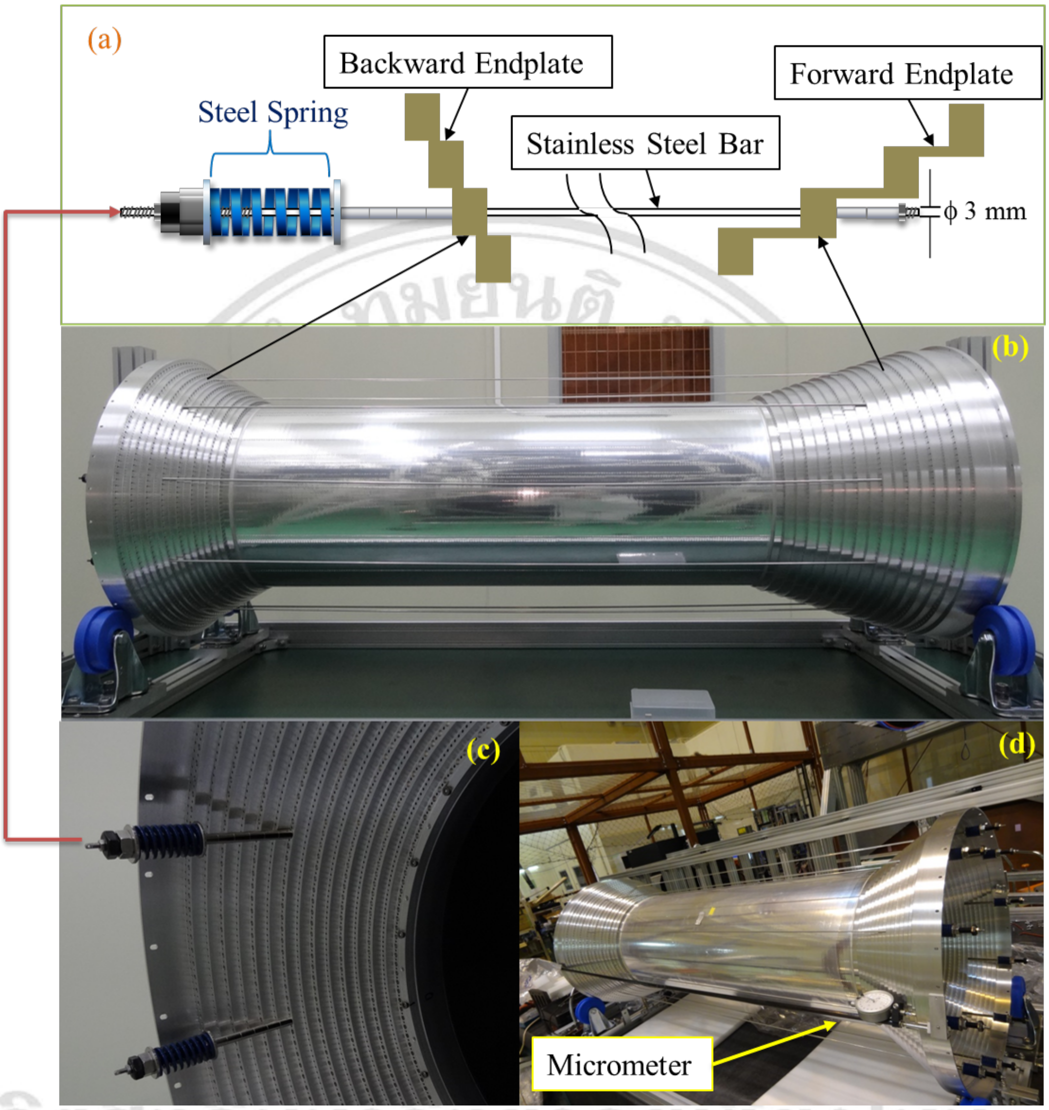

Figure 4.2: The chamber set up for tension load test,

(a) : The schematic diagram of the tension load test,
(b) : Back end of the chamber, which the stainless steel bars and the steel springs had strung for the test,
(c) : The micrometers were fixed to the chamber for measuring of ΔD,
(d) : The bars were still strung with approximately 160 kg tension until the wire stringing of this layer starts.

4.2 Wire Stringing

The 4.0 mm diameter Noryl feedthroughs were chosen to fix the wires and to isolate them from the ground potential. However, due to the limited space, only aluminum pins with 1.6 mm diameter are used to hold the field wires. There are three types of feedthroughs corresponding to the different geometry of each endplate as indicated in Figure 4.3. Since the pins were inserted into aluminum endplates directly, no additional connection to the ground is necessary.

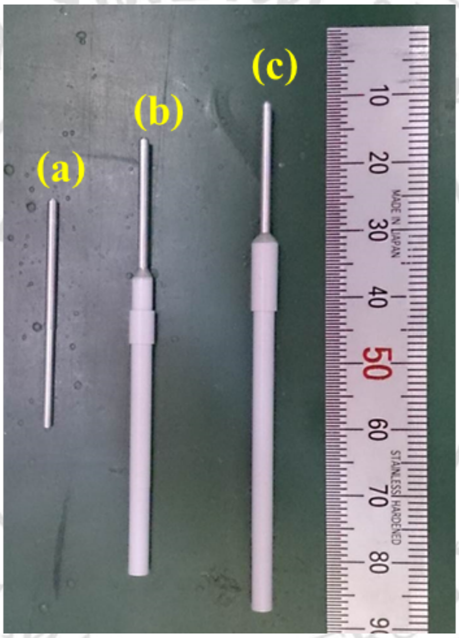

Figure 4.3: Three different types of feed troughs,

(a) : 1.6 mm diameter aluminum for every field wire in the inner chamber,
(b) : 4.0 mm diameter Noryl feedthrough for mounting the sense wire on the back end,
(c) : 4.0 mm diameter Noryl feedthrough for mounting the sense wire on the front end.

The inner chamber had its wires strung separately before installation into the main chamber. It is placed horizontally on the rollers in order to rotate the chamber as shown in Figure 4.2 (d). A wire spindle was set up on the front end side with low flexibility height, thus, the chamber had to be rotated until the target wire hole on the endplate are equal to the wire spindle height. Next step, the wire was pulled from the spindle through both endplates' holes and the feedthrough. Then, the feedthrough was inserted into the hole and was fixed by silicone for gas seal. On the front end, the wire was fixed by crimping

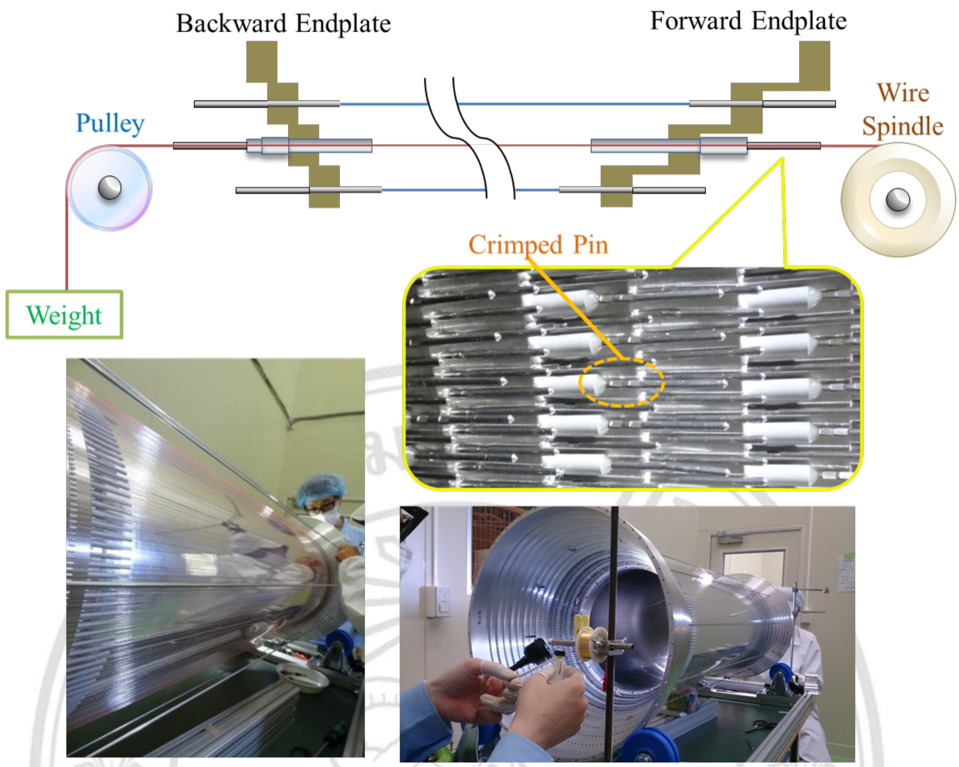

Figure 4.4: Overview of wire stringing process.

the crimping pin of the feedthrough with the air pressure crimp. The surplus wire was cut if it was out of the pin. On the back end, the wire was worn on a pulley and was connected to the weight pendulum, which the tension of 50 g was applied for the sense wire and 80 g for the field wire. Finally, the wire was fixed on the back end and was cut when it is out of the pin.

Because the length of the sense wire feedthrough is longer than the endplates' step size (Figure 4.5 (a)), it is impossible to crimp the field wire pin if the inner layer sense wire are already strung. Thus, the wire stringing of the field wire layer need to be finished before string the sense wire in previous inner layer. To avoid the crossing of sense wires, which is difficult to visually check, the pink Nylon wires called "dummy wires" are used to represent the positions of the sense wires (Figure 4.5 (b)). After finish the next layer field wire stringing, the dummy wires were connected to the sense wires on the front end and were pulled to the back end. Then, the tension of 50 g was applied and crimped.

The chamber and the fixture were placed in the clean room in which the air condition is controlled to keep the environment at the clean, constant temperature of 20 ^{o}C and at low

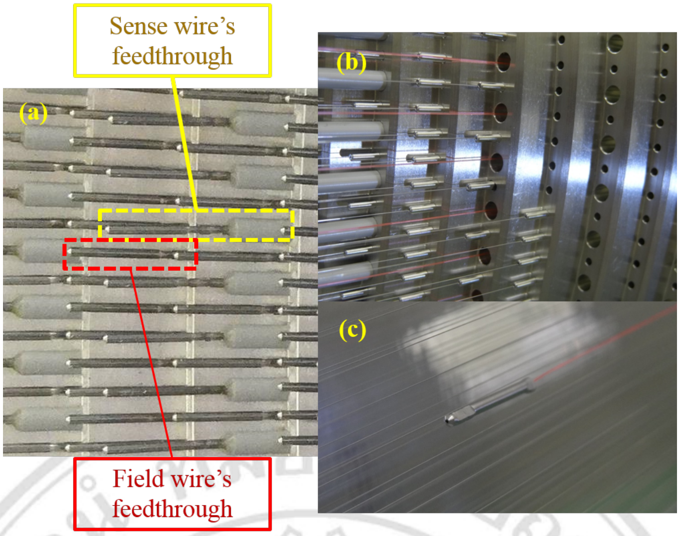

Figure 4.5: Sense wire stringing,

(a) : The length of the sense wire feedthrough is longer than the endplates' step size,
(b) : The dummy wires are used to represent the sense wire while the outer layer field wires are strung,
(c) : By connecting the sense wire to the dummy wire and by pulling it to the back end, the sense wires are strung without crossing.

humidity of less than 30%. Otherwise, the dust on the surface of the wire may causes the break down or the leak current and the aqua on the surface of the wire or the feedthrough tends to increase the dark current of the wire in the operation condition. The wire stringing began in the middle of April 2013 and finished at the beginning of June 2013.

4.3 Wire Tension Measurement

The tension of the sense wire was measuring by the resonant frequency of the wire oscillation in the magnetic field of the permanent magnet. The wire's tension in Newton (T) has relation with the resonance frequency of the wire oscillation as written,

$$T = \frac{4}{m^2} f^2 l^2 \rho \tag{4.1}$$

where:

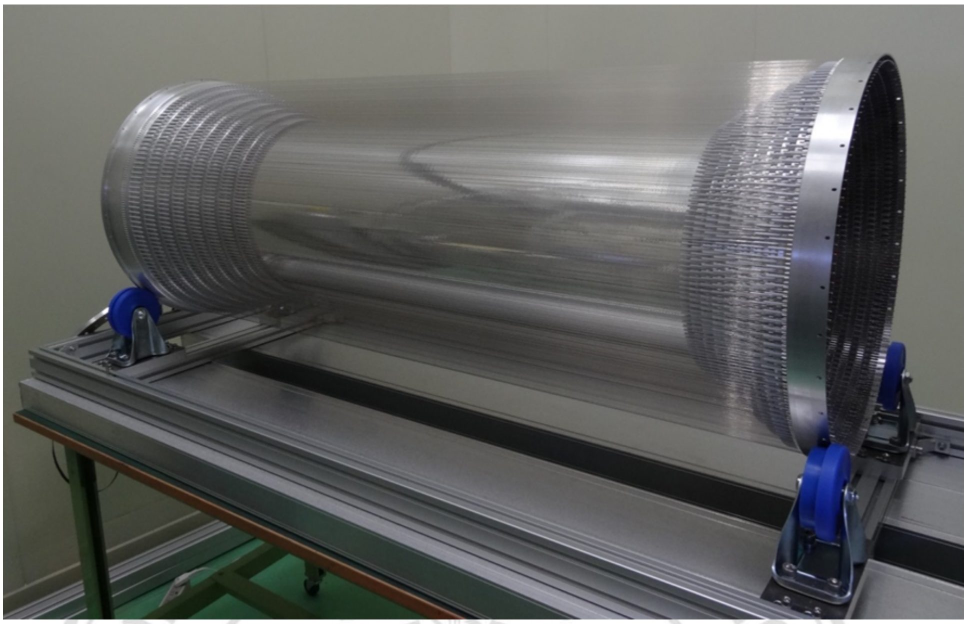

Figure 4.6: The inner chamber with the whole wires strung.

l : wire length in meter ,

ρ : linear density of the wire (Aluminum wire: 33 mg/m, Au-W wire: 13.5 mg/m),

f : resonance frequency in Hz,

m : mode number of resonance (m = 1, 2, 3, ...).

Figure 4.7 shows the setup of the tension measurement. The permanent magnet was put under the chamber in order to provide the magnetic field perpendicular to the wire length. The sinusoidal current was applied for making the wire to mechanical oscillate due to the Lorentz force caused by the magnetic field. At the same time, the movement of the wire in the magnetic field induced the current following the Faraday's law. The resonance frequency of the wire was searched by subtracting the input frequency from the monitoring of the current signal. The signal from the neighbor wire which shares the same layer, called the "reference", was also measured to improve the signal to noise ratio. The noisy phase was rejected by taking differential between the signal and reference. The error of this measurement was less than 0.6 % [6]. The distribution of the tension was fitted with Gaussian distribution and the wire with the tension less than 10 % from the center of the Gaussian distribution will be replaced. The tension data were used to calculate the wire position, which effects the precision of the track reconstruction.

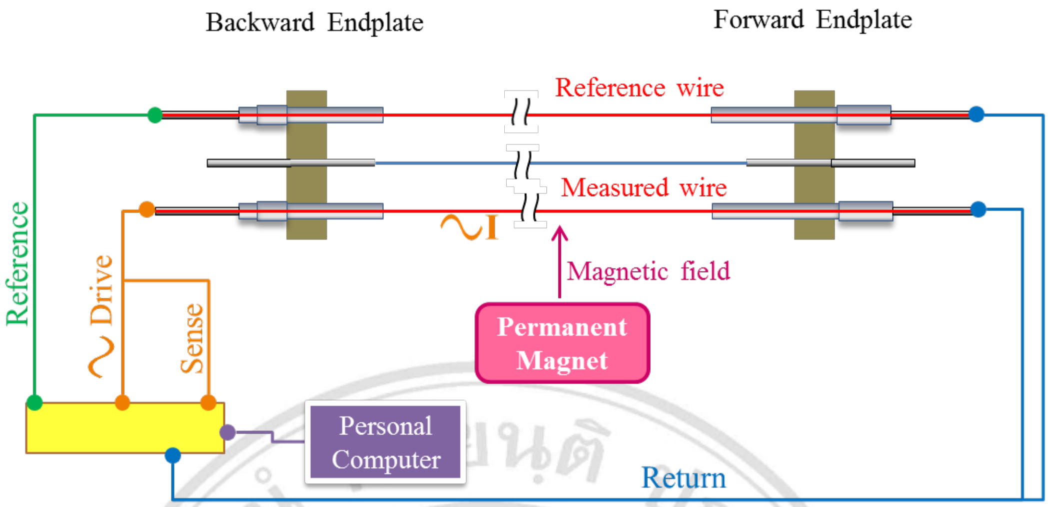

Figure 4.7: Setup for the tension measurement.

The tension of the field wires of the small cell chamber, which grounded to the end plate, is difficult to be measured. However, the low tension wire has to be checked and to be replaced by the new one with the proper tension. The Air flow was used to blow the field wires. Due to the large diameter of the field wire, the oscillation of the low tension wire was able to be easily detected by eyes.

The tension was measured layer by layer after the wire stringing of each layer was finished and it was re-checked after the whole wires were strung. Finally, the isolation of each sense wire from the end plate and from the connection of the field wire was checked.

4.4 Gas Leak Test

To check the gas seal potentiality, the inner chamber was inserted into a temporary aluminum cylindrical cover (Figure 4.8(a.)), which was removed before it was inserted to the main part. Then, the chamber was filled with Helium (He) gas (Figure 4.8(b.)). The GL Sciences Leak Detector LD229 was used to detect the He gas leak point (Figure 4.8(c.)). The glue, “lock-tite 222” 4.8(d.), was painted on the head of the crimp pin to seal the gas leak from the edge of the crimping pin. In addition, the silicone for the gas seal was added to some connections between the feedthroughs and the holes, where the large gas leak were found. All boundaries and joints were checked to stop the leak as well.

The helium gas was fed to the chamber until the relative pressure of the chamber reached approximately 100 mmH_2O per one atm room pressure. Then, the incoming and outgoing gas valves were closed. The gas pressure, which decreased due to the gas leak, was collected as the time dependence. These was used to calculate the leak rate of the gas. The connection between the inner cylinder and the back endplate was modified after the great amount of gas leak from the connection was found. Figure 4.9 shows the measurement results of the leak rate, which was improved day by day. The leak rate was measured as the time dependence of the pressure between the atmosphere and the pressure in the chamber. The improvement of the leak rate can be determined from the slope of the plot.

The leak rate of the chamber was approximately 5 cc/min at 100 mmH_2O relative pressure. The gas leak rate improvement was paused before starting the chamber test with the cosmic ray. The result of this test is presented in the next chapter. The gas leak test will be operated again after the inner chamber was inserted into the main chamber.

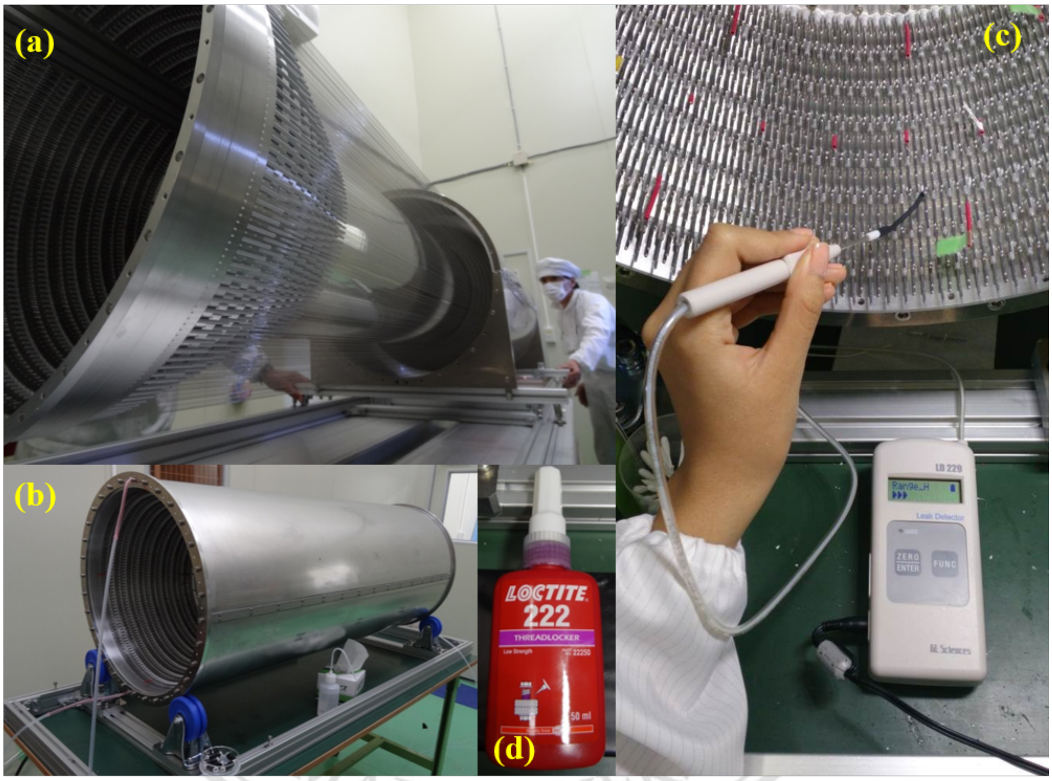

Figure 4.8: Gas leak rate of the inner chamber was checked. Sealing the leak was done to get the leak rate of 5 cc/min.

(a) : The inner chamber was inserted into the temporary aluminum cover,
(b) : The chamber was filled with Helium gas,
(c) : The gas leak check using GL Sciences He Gas Leak Detector LD229,
(d) : The glue ”lock-tite 222“ was used to seal the crimping pin.

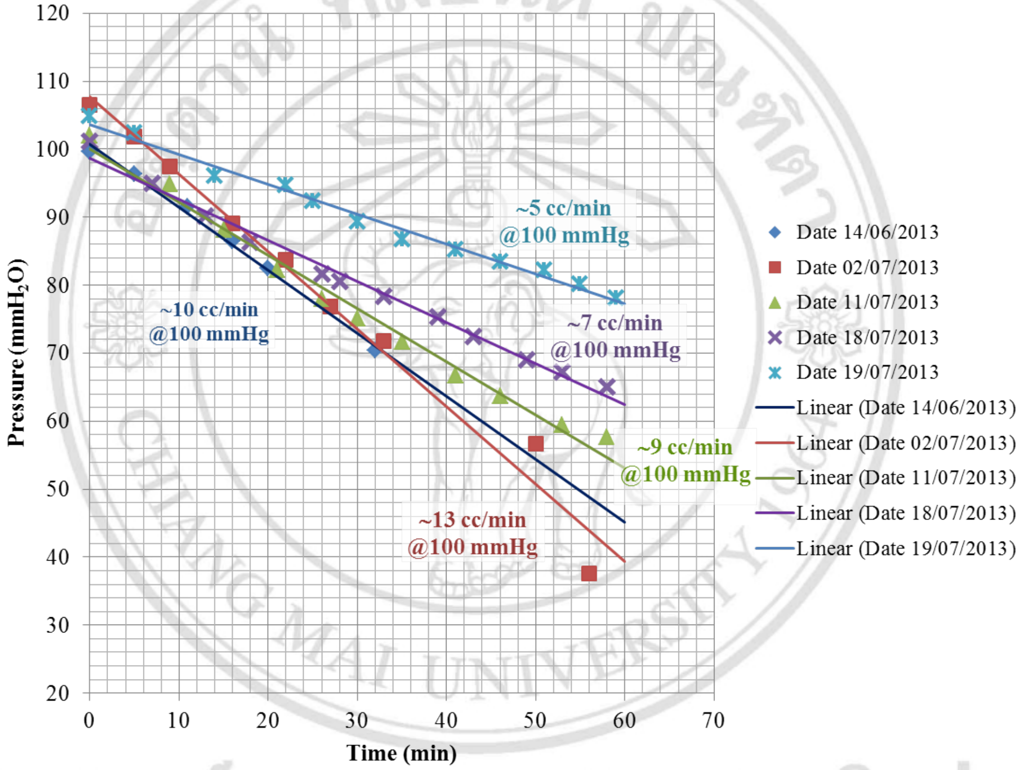

Figure 4.9: The measurement results of the leak rate.